JOURNAL OF APPLIED POLYMER SCIENCE VOL. 19, PP. 2107–2118 (1975)

Viscoelastic Analysis on Peel Adhesion of Adhesive Tape by Matrix Method

SHOOICHI YAMAMOTO and MASAHIKO HAYASHI, *Engineering Department, Nitto Electric Industrial Co., Ltd., Osaka, Japan,* and TATSUO INOUE, *Department of Mechanical Engineering, Kyoto University, Kyoto, Japan*

Synopsis

Analysis by means of matrix method is presented on the phenomenon of peel adhesion for 90° peeling of adhesive tape. A model of framed structure was assumed to duplicate the viscoelastic behavior of the tape: The adhesive layer is composed of a network structure made by elastic members for lattice elements and viscous members for diagonal elements. Calculated force distribution near the bond boundary showed good agreement with the experimental results of Kaelble. It was also found that the curve of peel rate versus peel force for the cohesive failure occurred in the adhesive layer was S-shaped; the change of peel force was affected severely by particular range of peel rate. For the interfacial failure at the bond boundary, on the other hand, the peel force possessed a maximum value for medium peel rate. Predicted failure mode for the adhesive tape changed from cohesive failure to interfacial failure with increasing rate of separation. Analytical results for the dependences of thickness of flexible members and adhesive layers on peel forces showed qualitative correlation with the experimental results.

INTRODUCTION

Evaluation of the characteristics of adhesive tape is often made by peel tests. The peel force acting on the flexible member is measured when the adhesive tape is removed from the adherend.

Surveying the test results performed over the years, several aspects have been pointed out: The bond stress distribution near the bond boundary between the adhesive and the adherend was measured by Kaelble.[1,2] For the dependence of peel rate on the peel force, it was reported that the peel force increases with increasing rate of peeling and decreases abruptly at a certain critical rate, and that the modes of failure change from cohesive to interfacial type.[2,3,4,6] With respect to the dependence of the thickness of the flexible member, the peel force increases with increasing thickness except for an extremely thick tape.[5,7] Similarly, the peel force increases with increasing thickness of adhesive layer.[6,7]

The extensive investigations for the analysis of peel adhesion, on the other hand, carried out by several researchers and the mechanism of peel adhesion have been clarified considerably.[1,8–15] However, discrepancy still exists between such theories of peel adhesion and experimental results. The authors proposed in this study a model of framed structure as a duplication of the adhesive tape, and analyses were performed by means of matrix method[16,17] for two cases; the adhesive layer only is peeled, and the adhesive tape consisted of adhesive layer and the flexible member is peeled. Calculations were also

made on the deformation of adhesive layer the interfacial force distribution, and the force distribution in the adhesive layer. Based on the analytical results, the mechanism of peel adhesion for 90° peeling was discussed. Moreover, we refer also to the dependence of viscoelastic properties of adhesive tape on peel force.

ANALYTICAL PROCEDURES

The framed structure model illustrated in Figure 1 is assumed for the adhesive layer, one of the components of adhesive tape. The model has two types of members: Elastic members with elastic modulus E arranged in parallel to x–y axes, and viscous members with viscosity η as the diagonal elements. For the sake of simplicity, individual members are pin-jointed at the nodes numbered in the figure, so that bending moments cannot be transmitted.

If we take the reference coordinate system x–y as shown in Figure 1, the stiffness relation of a typical elastic member is written as

$$\mathbf{X} = \mathbf{K}\mathbf{u} \tag{1}$$

where $\mathbf{X}$ is a force vector composed of forces X_{ij} and Y_{ij} in the x- and y-direction, respectively, acting on the node i–j, and $\mathbf{u}$ is a displacement vector whose components at that node are u_{ij} and v_{ij}. The elastic stiffness matrix is represented by $\mathbf{K}$ in eq. (1). For the nodes 1–1 and 1–2, with the cross-sectional area A and length L of the member, for example, eq. (1) may be reduced to

$$\begin{Bmatrix} X_{11} \\ Y_{11} \\ X_{12} \\ Y_{12} \end{Bmatrix} = \frac{AE}{L} \begin{bmatrix} 1 & 0 & -1 & 0 \\ 0 & 0 & 0 & 0 \\ -1 & 0 & 1 & 0 \\ 0 & 0 & 0 & 0 \end{bmatrix} \begin{Bmatrix} u_{11} \\ v_{11} \\ u_{12} \\ v_{12} \end{Bmatrix} \tag{2}$$

Next, formulation will be made on the viscous member by introducing the local coordinate system $\bar{x}$–$\bar{y}$ shown in Figure 1. In this system, we can write

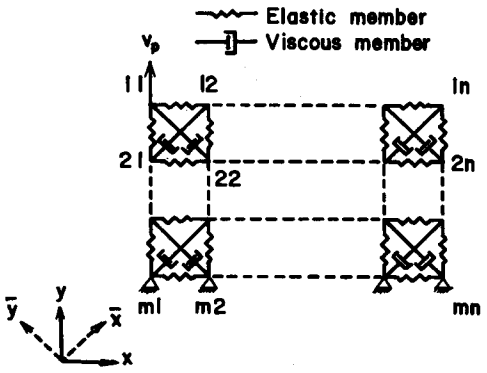

Fig. 1. Framed structure model for adhesive layer.

the relation between force and deformation rate of a typical viscous member in the form

$$\bar{\mathbf{X}} = \bar{\mathbf{V}} \frac{d\bar{\mathbf{u}}}{dt} \tag{3}$$

where $\bar{\mathbf{X}}$ and $d\bar{\mathbf{u}}/dt$ are vectors of nodal force and deformation rate, respectively, and $\bar{\mathbf{V}}$ is a matrix representing viscosity. The vectors of force $\mathbf{X}$ and deformation rate $d\mathbf{u}/dt$ in the reference system x–y can be obtained in terms of transformation matrix $\mathbf{T}$ as

$$\bar{\mathbf{X}} = \mathbf{T}\mathbf{X} \tag{4}$$

and

$$\frac{d\bar{\mathbf{u}}}{dt} = \mathbf{T}\frac{d\mathbf{u}}{dt}. \tag{5}$$

Substituting eqs. (4) and (5) into eq. (3) leads to

$$\mathbf{X} = \mathbf{T}'\bar{\mathbf{V}}\mathbf{T}\frac{d\mathbf{u}}{dt} = \bar{\mathbf{V}}\frac{d\mathbf{u}}{dt} \tag{6}$$

where $\mathbf{V}$ is given as

$$\mathbf{V} = \mathbf{T}'\bar{\mathbf{V}}\mathbf{T} \tag{7}$$

and $\mathbf{T}'$ stands for the transpose matrix of $\mathbf{T}$. As the cross-sectional area and the length of the viscous member in Figure 1 are A and $\sqrt{2}L$, respectively, eq. (6) for nodes 1–1 and 2–2, for example, can be written as follows:

$$\begin{Bmatrix} X_{11} \\ Y_{11} \\ X_{22} \\ Y_{22} \end{Bmatrix} = \frac{A\eta}{2\sqrt{2}L} \begin{bmatrix} 1 & -1 & -1 & 1 \\ -1 & 1 & 1 & -1 \\ -1 & 1 & 1 & -1 \\ 1 & -1 & -1 & 1 \end{bmatrix} \frac{d}{dt} \begin{Bmatrix} u_{11} \\ v_{11} \\ u_{22} \\ v_{22} \end{Bmatrix} \tag{8}$$

After evaluating eqs. (1) and (6) for each elastic and viscous member, the overall system of equations can be obtained by superposing these quantities:

$$\mathbf{X}_s = \mathbf{K}_s\mathbf{u}_s + \mathbf{V}_s\frac{d\mathbf{u}_s}{dt} \tag{9}$$

where the matrices with symbol S denotes the overall matrices. In order to solve the linear differential equation by finite difference scheme, the subscript of time t should be attached as follows:

$$(\mathbf{X}_s)_t = \mathbf{K}_s(\mathbf{u}_s)_t + \mathbf{V}_s\left(\frac{d\mathbf{u}_s}{dt}\right)_t. \tag{10}$$

Linear variation of term $d\mathbf{u}_s/dt$ is assumed during the time interval Δt, and we have the equations

$$(\mathbf{u}_s)_t = (\mathbf{u}_s)_{t-\Delta t} + \left\{\left(\frac{d\mathbf{u}_s}{dt}\right)_{t-\Delta t} + \left(\frac{d\mathbf{u}_s}{dt}\right)_t\right\}\frac{1}{2}\Delta t \tag{11}$$

or

$$\left(\frac{d\mathbf{u}_s}{dt}\right)_t = -\left(\frac{d\mathbf{u}_s}{dt}\right)_{t-\Delta t} + \{(\mathbf{u}_s)_t - (\mathbf{u}_s)_{t-\Delta t}\}\frac{2}{\Delta t}. \quad (12)$$

Substituting eq. (12) into eq. (10) leads to the following recursion formula:

$$\left\{\mathbf{K}_s + \frac{2}{\Delta t}\mathbf{V}_s\right\}(\mathbf{u}_s)_t = \mathbf{V}_s\left\{\frac{2}{\Delta t}(\mathbf{u}_s)_{t-\Delta t} + \left(\frac{d\mathbf{u}_s}{dt}\right)_{t-\Delta t}\right\} + (\mathbf{X}_s)_t. \quad (13)$$

Thus, $\mathbf{u}_s$ at time t can be evaluated by solving the system of simultaneous equations provided that the values of $\mathbf{u}_s$ and $d\mathbf{u}_s/dt$ are known at the preceding time step $t-\Delta t$. From the initial condition, the values of $d\mathbf{u}_s/dt$ can be determined from eq. (10) as follows:

$$\mathbf{V}_s\left(\frac{d\mathbf{u}_s}{dt}\right)_{t=0} = -\mathbf{K}_s(\mathbf{u}_s)_{t=0} + (\mathbf{X}_s)_{t=0}. \quad (14)$$

Substituting eq. (14) into eq. (13), the recursion formula of eq. (13) can be solved for the unknown displacement $(\mathbf{u}_s)_t$, and we can easily have the nodal forces and the internal forces in the members. Though the present analysis is based on the infinitesimal strain theory, approximate result of finite deformation may be obtained by the successive processes that the coordinates x_i–y_i and the lengths of all members are modified by using the determined displacement in each time step. Consideration of the variation of cross-sectional area are also included with the assumption that the material is incompressible.

In most peel tests, the peel forces are measured under the conditions of the prescribed peel rates (deformation rates). As the first step of an analogy of such peel test, the model in Figure 1 is settled in which the adhesive layer is stuck on the adherend and is peeled at right angle. The purpose of the present analysis is to determine the unknown nodal force Y_{11} under the prescribed value of constant nodal displacement rate dv_{11}/dt of the node 1–1, and the correlation between Y_{11} and dv_{11}/dt instead of that between the peel force P and the peel rate v_p will be discussed. The situation that the adhesive layer is stuck on the adherend is expressed by the condition that the displacements at the nodes $m1, m2, \ldots, mn$, in the figure, are constrained in both the x- and y-directions. If we perform the analysis under the above boundary conditions, the following data will be obtained: The nodal forces Y_{11} and Y_{mi} $(i = 1, 2, \ldots n)$, which represent the peel force and interfacial forces, respectively, the displacements of the nodes corresponding to the deformation of adhesive layer, and finally the internal forces in all members composing the adhesive layer.

In addition to such data, the phenomenon of the failure of adhesive tape was discussed. As the failures generally occur in the adhesive layer or at the boundary between the layer and the adherend, we denote the former as cohesive failure and the later as interfacial failure. Assumptions are made here that the cohesive failure is due to the criterion that the internal force of a member reaches a critical value and that the interfacial failure is caused when the nodal force Y_{mi} $(i = 1, 2, \ldots, n)$ reaches a prescribed value.

The same procedure of the analysis on the adhesive layer may be available to discuss the mechanical behavior of the adhesive tape containing two layers

of the flexible member and the adhesive. In this case, the mechanical properties of the elastic modulus and the viscosity coefficient should be reduced to be different in both layers, and the calculation due to the matrix method should be carried out.

CALCULATED RESULTS AND DISCUSSION

Peel Adhesion of Adhesive Layer

Calculations of the interfacial force distribution and the force distribution in the adhesive layer as well as the deformation mode were carried out when only the adhesive layer is peeled for the first approximation of the peel adhesion of the tape. Discussion of the relations between the peel rate and the peel force for interfacial and cohesive failure is also included. In the present analysis, the adhesive layer is divided into 45 square elements with 16 nodes in the x-direction ($n = 16$) and four in the y-direction ($m = 4$). In order to perform calculations concretely, for instance, data were employed as follows: cross-sectional area A of each member, $A = 1$ mm^2; length of elastic member, $L_E = 1$ mm^2; length of viscous member, $L_\eta = \sqrt{2}$ mm^2; elastic modulus of elastic member, $E_a = 1$ kg/mm^2; viscosity coefficient of viscous member, $\eta_a = 1$ kg·sec/mm^2, respectively.

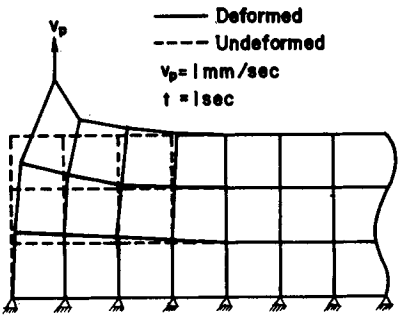

Fig. 2. Deformation mode of adhesive layer.

The calculated result of the deformation mode for adhesive layer is shown in Figure 2 at $t = 1$ sec subjected to constant peel rate of 1 mm/sec. The figure seems to reflect fairly well the deformation in actual peel test.

Figure 3 represents the distribution of forces, Y_{mn} (Y_{41}, Y_{42}, ..., Y_{4n}), along the interface between the adhesive layer and the adherend at several elapsed times. The maximum value of the interfacial force is observed at the peel end, and the distributions of interfacial forces vary with time, owing to the viscosity. Such forces may affect the predominant influence on the interfacial failure to be discussed later.

In order to discuss the force distribution in the adhesive layer, consider the elastic members arranged vertically to the interface, which affect the remarkable influence on the peel adhesion. The internal force distributions in the adhesive layer are shown in Figure 4. The hollow circles in the figures correspond to the values in the elastic members arranged vertically in the top row of Figure 1, as the forces play an important role in the cohesive failure.

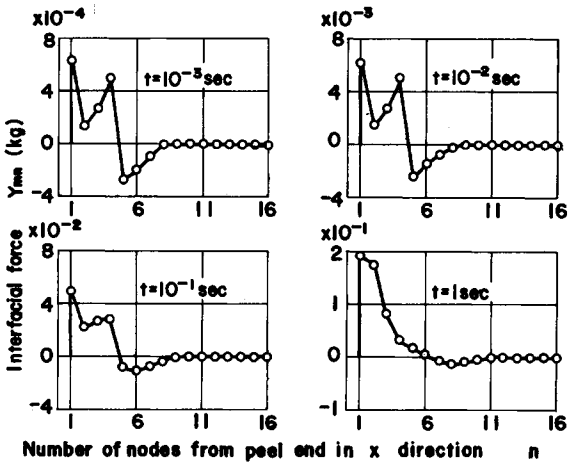

Fig. 3. Distribution of interfacial forces in adhesive layer.

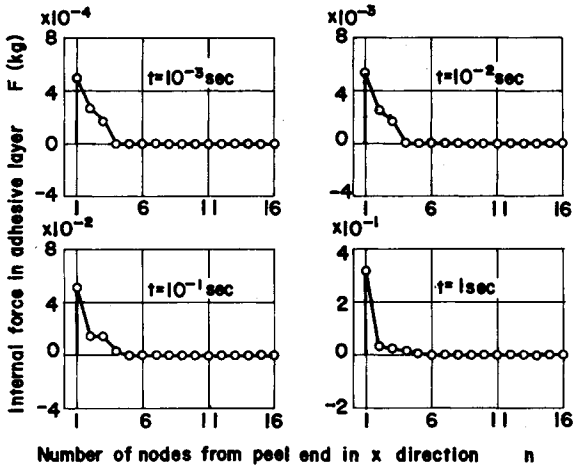

Fig. 4. Internal force distribution in adhesive layer.

The calculated result on the interfacial force may provide interesting information on the mechanism of the interfacial failure. The interfacial forces are increased predominantly with increasing time, as shown in Figure 3. An assumption is made here that the failure occurs at the interface when the maximum value among the forces Y_{41}, Y_{42}, ..., Y_{4n} reaches a prescribed critical value $(Y_c)_i$ and that the nodal force Y_{11} for such a case corresponds to the peel force, where the critical force is assumed to be independent of peel rate. The thus obtained relation between the peel rate and the peel force is illustrated in Figure 5a for $(Y_c)_i$ = 0.02 kg. The curve possesses a maximum value at medium peel rate, while the rate dependence on the peel force is small at low or high peel rate.

Next, attention is focused on the cohesive failure mode, especially the dependence of peel rate on the peel force. Failure criterion in this case is assumed as follows: Failure in the adhesive layer occurs when the internal

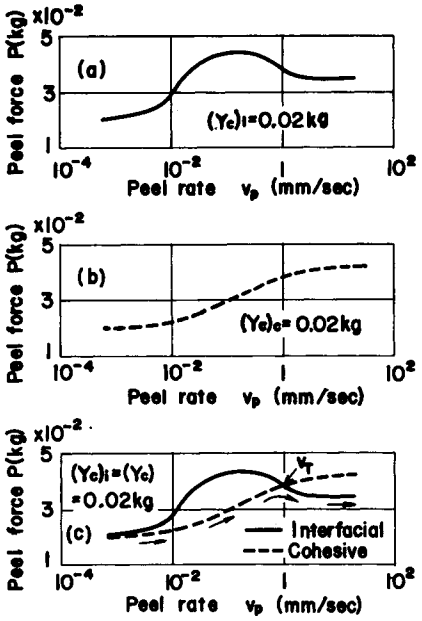

Fig. 5. Transition from cohesive failure to interfacial failure in adhesive layer: (a) peel curve for interfacial failure; (b) peel curve for cohesive failure; (c) superposed result of the above two curves.

force in a member reaches a critical value $(Y_c)_c$. The relation between the peel rate and the peel force for the cohesive failure obtained by the above-mentioned procedure is shown in Figure 5b with a critical fracture force $(Y_c)_c$ of 0.02 kg. The shape of this curve is somewhat different from that in Figure 5a, where the peel force increases monotonously with increasing rate of separation.

Finally, the transition of failure mode from cohesive to interfacial will be suggested as transition phenomena are observed in some peel tests. If we superposed the curves in Figures 5a and 5b for the case $(Y_c)_i = (Y_c)_c = 0.02$ kg, the actual failure will be determined by the lower curve in Figure 5c. The cohesive failure (broken line) occurs predominantly in the region of low peel rate, while the peeling is dominated by the interfacial failure (solid line) for higher peel rate than a transition point v_T.

Peel Adhesion of Adhesive Tape

The adhesive tape composed of two layers (adhesive layer and flexible member) with different mechanical properties will be treated in this section. The model of adhesive tape as shown in the broken line in Figure 6 is constructed by the flexible member with three square elements in thickness attached to the adhesive layer in Figure 1. The mechanical properties employed in this analysis are listed in Table I, where both elastic modulus E_b and viscosity coefficient η_b of the flexible member are large enough compared with those of the adhesive layer. The solid line in Figure 6 gives an example of the consequence of deformation of the adhesive tape at $t = 1$ sec with a constant peel rate of 1 mm/sec. As is seen in this figure, the deformation of

TABLE I
Mechanical Properties of Adhesive Tape

	Elastic modulus, kg/mm²	Viscosity coefficient, kg·sec/mm²
Flexible member	$E_b = 100$	$\eta_b = 100$
Adhesive layer	$E_a = 1$	$\eta_a = 1$

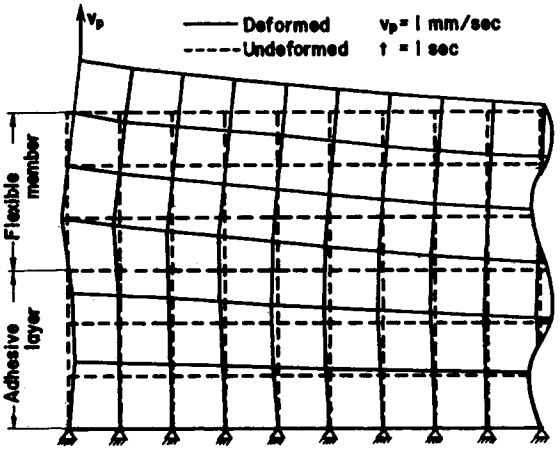

Fig. 6. Deformation mode of adhesive tape.

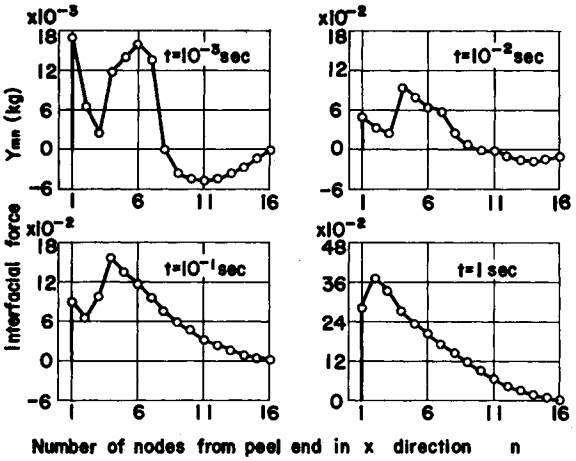

Fig. 7. Distribution of interfacial forces in adhesive tape.

adhesive layer is large, especially in the neighborhood of the peel end, while the flexible member is bent slightly due to the large moduli of elasticity and viscosity. Distributions of force at the interface between the adhesive layer and the adherend are shown in Figure 7 with parameters of time elapsed. The peak of the interfacial force in this case is observed in the internal region, while the force for only the adhesive layer has a maximum at the end of the layer, as already discussed in Figure 3. Such an analytical result of the

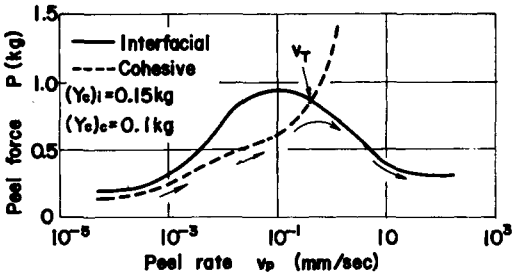

Fig. 8. Transition from cohesive failure to interfacial failure in adhesive tape.

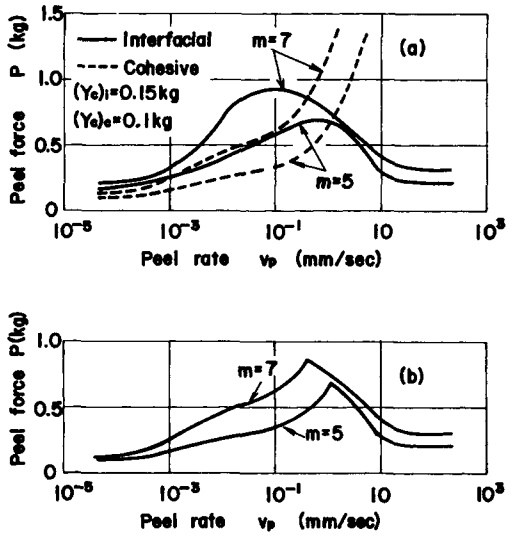

Fig. 9. Dependence of thickness of flexible member on peel curve: (a) interfacial and cohesive failures for flexible members with different thicknesses; (b) peel curves for flexible members with different thicknesses.

distribution of interfacial force reflects the experimental one obtained by Kaelble.[1,2]

The transition phenomenon from cohesive failure to interfacial of the tape with two layers may be clarified by the same discussion previously made of the case without flexible member. The calculated peel forces in the cases of interfacial and cohesive failures are shown in Figure 8 versus the peel rate. A transition analogous to Figure 5c of the mechanism of failure is observed, while the peel curve for cohesive failure diverges at high peel rate. The peel curve assigned by arrows reflects the qualitative results of the experiments.[4]

In order to investigate the dependence of the thickness of the flexible member to the peel force, we employed several models of adhesive tape with different numbers of square elements. The mechanical properties of two layers and also the thickness of the adhesive layer were unchanged. The solid and the broken lines in Figure 9a correspond to the analytical results of peel force for the interfacial and the cohesive failure mode, respectively, with the parameter of numbers of total nodes m in the y-direction, where the criti-

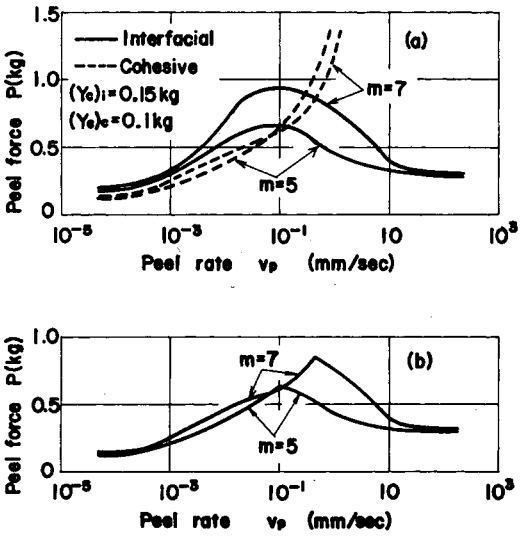

Fig. 10. Dependence of thickness of adhesive layer on peel curve: (a) interfacial and cohesive failures for adhesive layers with different thicknesses; (b) peel curves for adhesive layers with different thicknesses.

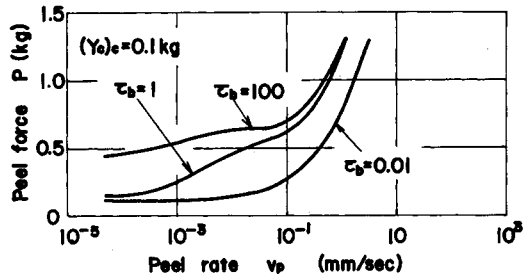

Fig. 11. Influence of relaxation time on cohesive failure curve for flexible member.

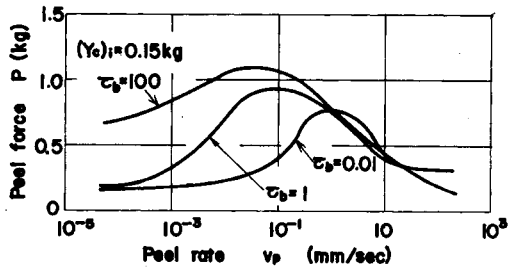

Fig. 12. Influence of relaxation time on interfacial failure curve for flexible member.

cal forces for interfacial and cohesive failure are taken as 0.15 kg and 0.1 kg. The practical peel curves, including the effect of transition phenomena, are illustrated in Figure 9b. The tendency that the peel force increases with thickness of the flexible member as is observed generally in most peel test[5,7] is to be recognized from the analytical results.

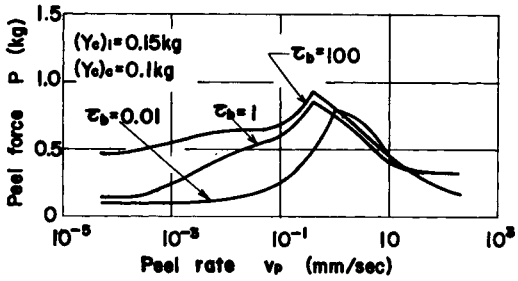

Fig. 13. Influence of relaxation time on peel curve for flexible member.

The dependence of the thickness of adhesive layer on the peel force can be examined, on the other hand, by employing the models in which the adhesive layers are divided into the sequences of one or three square elements.

Figures 10a and 10b show the results of analyses representing the influence of the thickness of layer, while the flexible member has constant three elements in the y-direction. The qualitative characteristics that the peel force increases with the thickness of the adhesive layer[6,7] is also clarified from these figures.

The influence of mechanical properties of the material of the flexible member is discussed as follows: Viscosity coefficients η_b of 1,100 and 10,000 kg·sec/mm^2 with constant elastic modulus E_b of 100 kg/mm^2 are employed for the calculation of peel force. The relaxation time τ_b (= η_b/E_b) is introduced as a parameter of the mechanical property instead of the viscosity coefficient. The model of the tape used is the same as that shown in Figure 6.

Figures 11 and 12 represent the effects of the relaxation time (τ_b = 0.01, 1, 100 sec) on the peel force in the cases of cohesive and interfacial failure, respectively. In the case of cohesive failure, the peel force with large relaxation time remains constant in some region of the peel rate, as is seen in Figure 11. Such an effect is often called "shoulder" and is observed in some peel tests.

It is also found from Figure 12 that the peel rate when the peel force is maximum is reduced to shift to the lower side with increasing relaxation time when the peeling of the tape is dominated by interfacial failure. The estimated peel curve may be obtained as shown in Figure 13 by superposing the peel forces in Figures 11 and 12, and we obtain the interesting information that the peel force is affected remarkably by the mechanical properties of the flexible member only at low peel rate.

CONCLUSIONS

In order to investigate the mechanical behavior of the adhesive tape, the authors proposed a viscoelastic model consisting of a framed structure with elastic and viscous members, and calculations in terms of matrix method were applied to the model.

Detail discussions were carried out, at the first stage, on the adhesive layer, followed by analyses of the tape with flexible member.

The present analyses led to transition phenomena from cohesive failure to interfacial failure. The effects of the thickness of flexible member and adhe-

sive layer on the peel force were discussed, and attention was paid also to the effect of the mechanical properties of materials of the tape.

The analytical results for several characteristics of the tape were in good correlation with the behavior observed in most experiments.

The main conclusion obtained is that such an analytical method by using the proposed viscoelastic model may provide instructive information for designers of adhesive tapes.

References

1. D. H. Kaelble, *Trans. Soc. Rheol.*, **9**, 135 (1965).
2. D. H. Kaelble and R. S. Reylek, *J. Adhes.*, **1**, 124 (1969).
3. D. H. Kaelble, *J. Adhes.*, **1**, 102 (1969).
4. A. N. Gent and R. P. Petrich, *Proc. Roy. Soc. A*, **310**, 433 (1969).
5. D. Satas and F. Egan, *Adhes. Age*, 22 (Ausust 1966).
6. J. L. Gardon, *J. Appl. Polym. Sci.*, **7**, 625 (1963).
7. J. Johnston, *Adhes. Age*, 20 (April 1968).
8. J. J. Bikerman, *J. Appl. Phys.*, **28**, 1484 (1957).
9. F. S. C. Chang, *Trans. Soc. Rheol.*, **4**, 75 (1960).
10. S. Yurenka, *J. Appl. Polym. Sci.*, **6**, 136 (1962).
11. J. L. Gardon, *J. Appl. Polym. Sci.*, **7**, 643 (1963).
12. T. Hata, *J. Soc. Mater. Sci. Japan*, **13**, 341 (1964).
13. Y. Nonaka, *J. Adhes. Soc. Japan*, **1**, 319 (1965).
14. T. Hata, *J. Adhes.*, **4**, 161 (1972).
15. T. Igarashi, *J. Adhes. Soc. Japan*, **8**, 250 (1972).
16. H. C. Martin, *Introduction to Matrix Methods of Structural Analysis*, McGraw-Hill, New York, 1966.
17. O. C. Zienkiewicz and Y. K. Cheung, *The Finite Element Method in Structural and Continuum Mechanics*, McGraw-Hill, New York, 1967.